



1 Porosity of recycled concrete with substitution
2 of recycled concrete aggregate
3 An experimental study

4 José M.V. Gómez-Soberón*

5 3 Sur #503 Cd. Serdán, Puebla, CP 75520, Mexico

6 Received 8 June 2001; accepted 5 March 2002

8 **Abstract**

9 In this paper, we present the experimental analysis of samples of recycled concrete (RC) with replacement of natural aggregate (NA) by
10 recycled aggregate originating from concrete (RCA). The results of the tests of mechanical properties of RC were used for comparison with
11 tests of mercury intrusion porosimetry (MIP), in which the distribution of the theoretical pore radius, critical pore ratio, the surface area of the
12 concrete, threshold ratio and average pore radius were studied at ages of 7, 28 and 90 days. The results showed some variation in the
13 properties of the RC with respect to ordinary concrete. Porosity increases considerably when NA is replaced by RCA. Additionally, a
14 reduction in the mechanical properties of the RC is seen compared with ordinary concrete when porosity increases. © 2002 Published by
15 Elsevier Science Ltd.

16 *Keywords:* Compressive strength; Porosity; Recycled concrete; Recycled concrete aggregate; Young's modulus

17
18 **1. Introduction**

19 Current studies of recycled concrete (RC), with partial
20 substitution of natural aggregate (NA) by recycled aggregate
21 originating from concrete (RAC), promise a feasible path
22 for its application, thus satisfying a need, saving energy,
23 improving environmental conditions and providing a solu-
24 tion for the 200 million tons/year of construction waste
25 generated in the EU [1–7].

26 RCs can be regarded as porous concretes, having per-
27 meability values that are twice those of ordinary concretes.
28 Their general behavior shows a decrease in their mechanical
29 and physical properties as the percentage of replacement of
30 NAs by RCA increases [8]. It is also widely accepted that
31 there is an inverse correlation between the volume of pores
32 and the levels of stress to which the concrete can be
33 subjected, and this relationship should also take into account
34 the distribution of the sizes of the pores and the intercon-
35 nection between them [9–11].

36 Tests of mercury intrusion porosimetry (MIP) in RC 36
37 show increases in the total volume of pores, especially in 37
38 larger pores (>100 nm). This suggests that this property is a 38
39 function of both the age of the concrete and the amount of 39
40 mortar that the RCA contains [12]. 40

41 Five types of concrete are presented in this work with 41
42 different RCA contents, together with the behavior of the 42
43 concrete that provided the RCA, and were prepared for 43
44 the study of the properties of both the aggregates and 44
45 the concretes. 45

46 **2. Experimental**

47 *2.1. Original concrete*

48
49 In this study, 4 m³ of original concrete (OC) was used. 49
50 The concrete was made in a mixer and was poured into 50
51 wooden formwork frames measuring 0.40 × 0.20 × 0.10 m. 51
52 Fifty cylinders measuring Ø 0.15 × 0.30 m, eight measuring 52
53 Ø 0.15 × 0.45 m and four cubes measuring 0.10 × 0.10 m 53
54 were also used to study the porosity, mechanical behavior, 54
55 shrinkage and creep. 55

* L'Hospitalet de Llobregat, Av. Carrilet #338 5-3, Barcelona 08901
Spain. Tel.: +34-933-37-05-69; fax: +34-934-01-72-62.

E-mail address: jmv115@hotmail.com (J.M.V. Gómez-Soberón).

t1.1 Table 1

t1.2 Mixtures used for OC

Component	OC
t1.4 Cement (kg/m ³) ^a	380
t1.5 Water (kg/m ³)	168
t1.6 Fine gravel (5–12) (kg/cm ³) ^b	252
t1.7 Gravel (12–20) (kg/cm ³) ^b	773
t1.8 Sand (0–5) (kg/m ³) ^b	784
t1.9 W/C	0.44
t1.10 Coarse A/Fine A (vol)	1.3
t1.11 Additives (plastifier)	2.69

t1.12 ^a CEM I 42.5 R.

t1.13 ^b Limestone aggregate, Garraf quarry, Barcelona.

56 Twenty-four hours after pouring, the samples were
 57 removed from the formwork and submitted to a curing
 58 process for 150 days (see Table 1, in which the specific
 59 characteristics of this concrete are given). The specimens
 60 were then passed once through a semifixed roller grinder
 61 with an inlet width of 0.45 m and a maximum outlet size of
 62 0.025 m. Finally, the resulting material was classified into
 63 sizes (mm in all cases): 0–5, 5–10, 10–20, 20–25. The 5–
 64 10 and 10–20 fractions were used as RCA in this work.

66 *2.2. Recycled aggregate and NA*

67 The designation used by sizes was: for RCA, gravel 10–
 68 20 and fine gravel 5–10; and for the NA, gravel 12–20 and
 69 fine gravel 5–12.

70 The criterion used for this fit was the compacted max-
 71 imum density (which reduced the possible influences of
 72 different particle size). These were:

- 73 • For RCA, the combination was 55% gravel and 45%
 74 fine gravel.
- 75 • For NA, the combination was 70% gravel and 30%
 76 fine gravel.

78 Table 2 shows the properties of the aggregate used. The
 79 total porosity to water is the variable that shows the greatest
 80 difference between the RCA and NA and, in the worst case,
 81 reaches 2.82% for the NA and 14.86% for the fine gravel
 82 fraction of the RCA. As regards density, the RCA is lighter

t2.1 Table 2

t2.2 Properties of recycled aggregate and NA

Property	RCA			NA ^a		
	10–20	5–10	0–5	12–20	5–12	0–5
t2.5 Dry specific gravity (kg/m ³)	2280	2260	2170	2570	2640	2570
t2.6 Specific gravity (surface dry) (kg/m ³)	2410	2420	2350	2590	2670	2600
t2.7 Water absorption (%)	5.828	6.806	8.160	0.876	1.134	1.49
t2.8 Total porosity (%)	13.42	14.86	–	2.70	2.82	–
t2.9 Shape coefficient	0.363	0.466	–	0.364	0.576	–
t2.10 Longs indices	6	15	–	8	19	–
t2.11 Modulus of fineness	7.2	6.2	3.8	6.9	5.0	3.3
t2.12 Sand equivalent (%)	–	–	93.6	–	–	93.8
t2.13 Particles <200 μm (%)	0.06	0.29	9.85	0.50	2.46	9.24

t2.14 ^a Limestone aggregate, Garraf quarry, Barcelona.

than the NA (with an average of 14% less in D_s and 9% less
 in D_{ss} .) The RCA shows an increase in density, which is
 directly proportional to the greater particle size. Finally, the
 differences between dry and dry surface saturated conditions
 are greater for the RCA than for the NA.

The RCA used in this study can be considered as being
 within the RILEM recommendation for Type II RCA
 (absorption $\leq 10\%$ and $D_s \geq 2000$ kg/m³). For the Belgian
 recommendation, they are GBSBII (absorption $< 9\%$ and
 $D_s > 2100$ kg/m³) and in the Japanese case they comply with
 the absorption requirement ($\leq 7\%$ and $D_s \geq 2200$ kg/m³) in
 the fractions used [13–16]. Consequently, the RCA
 employed in this study may be used in both plain and
 reinforced concrete if its application and factors of behavior
 are taken into account.

2.3. Mix of RCs

Due to the difficulty in determining the real water/
 cement (W/C) ration because of the high variation of
 absorption in the RCA, it was decided to use basic ACI
 211.1 and ACI 211.2 mix concepts in accordance with the
 following criteria.

(1) The substitution of NA by RCA was done using equal
 volume fractions with the following condition:

$$r = \frac{RCA_{coarse}}{RCA_{coarse} + NA_{coarse}}$$

$$(0.00 \leq r \leq 1.00)$$

where: r = percentage of NA replaced by RCA, by volume;
 RCA_{coarse} = 55% recycled gravel + 45% recycled fine
 gravel; and NA_{coarse} = 70% natural gravel + 30% natural
 fine gravel.

The percentages of the five studied samples of RC were:
 $r = 0.00, 0.15, 0.30, 0.60$ and 1.00 . As fine aggregate, 100%
 crushed natural limestone sand from the Garraf quarry
 (Barcelona) was used.

(2) The RCA showed an increase in absorption propor-
 tional to the time spent in water. The time allowed for the
 mixture was 20 min of immersion, with up to 97% fine gravel
 and 77% gravel, in all cases with comparison after 24 h.

Component		$r=1.00$	$r=0.60$	$r=0.30$	$r=0.15$	$r=0.00$
t3.1	Table 3					
t3.2	Mixtures used for RC					
t3.4	Cement (kg/m ³) ^a	400				
t3.5	Water (kg/m ³)	207.6				
t3.6	RCA (kg/cm ³)					
	Fine gravel (5–10)	406	258	134	69	0
t3.7	Gravel (10–20)	497	315	164	84	0
t3.8	NA (kg/cm ³)					
	Fine gravel (5–12) ^b	0	268	488	604	710
t3.9	Gravel (12–20) ^b	0	115	209	259	304
t3.10	Sand (0–5) (kg/m ³) ^b	662				
t3.11	W/C	0.52				
t3.12	Coarse A/Fine A (vol)	1.53				
t3.13	^a CEM I 52.5R UNE 80 301 96 RC/97.					
t3.14	^b Limestone aggregate, Garraf quarry, Barcelona.					

(3) The amount of water absorbed by the aggregate was taken into account separately, in addition to its wetness before mixing and the free water that formed part of the mixture. The above aspect is justified by criteria that were emphasized in a previous publication of the authors [17–20]. With the established mixing time and the required amount of water, the order of mixing the materials guaranteed (as far as possible) the immobility of the water and an improvement in the transition zone. The following sequence was adopted: (a) all of the coarse aggregates and water were introduced into the mixer; (b) these were mixed for 2 min; (c) the mixer was switched off for 3 min; (d) stages (b) and (c) were repeated twice; (e) the cement was introduced and mixed for 3 min; and (f) the sand was added and mixed for another 3 min.

The mixes obtained using the above criteria are given in Table 3. As can be seen, the variation in consistency and volumetric weight for the different percentages of aggregate replaced is within tolerable limits (slump 0.1 ± 0.03 m and concrete with volumetric weight normal).

t4.1 Table 4
t4.2 Mechanical and physical properties of RC

Age ^a factor	Tensile strength (MPa)			Compressive strength (MPa)			Young's modulus (GPa)			Absorption (%)	Water porosity (%)	D_s (kg/m ³)	D_{sss} (kg/m ³)	
	7	28	90	7	28	90	7	28	90					
t4.5	$r=0.00$	3.6	3.7	3.9	33.3	39.0	42.1	27.6	29.7	32.4	8.40	18.0	2130	2310
t4.6	$r=0.15$	3.3	3.7	3.9	33.9	38.1	41.6	27.2	29.1	30.1	8.60	18.5	2140	2360
t4.7	$r=0.30$	3.3	3.6	3.9	34.8	37.0	39.5	26.5	27.8	29.4	8.60	18.5	2150	2330
t4.8	$r=0.60$	3.2	3.4	3.7	30.6	35.8	38.3	25.5	26.6	27.6	9.00	19.2	2120	2320
t4.9	$r=1.00$	3.5	3.3	3.6	30.7	34.5	37.5	26.9	26.7	26.4	9.60	20.1	2090	2290
t4.10	OC	3.2	3.8	–	35.2	38.4	–	33.0	33.7	–	5.90	13.4	2270	2410
t4.11	OC ^b	4.1	4.1	4.2	45.1	45.4	47.0	35.2	34.5	34.6				

t4.12 ^a Days.
t4.13 ^b At 172, 179, and 262 days of age.

2.4. Properties of the concretes

The tests on the different concretes comprised the study of the physical properties such as absorption, density, porosity and water permeability; and mechanical properties such as compression, tensile strength, Young's modulus, shrinkage and creep.

Tests of the physical properties of the concrete were carried out on 0.10×0.10 m cubic samples, while the mechanical tests were done on $\emptyset 0.15 \times 0.30$ m (compression, tensile strength and Young's modulus) and $\emptyset 0.15 \times 0.45$ m cylindrical (shrinkage and creep) samples with ages of 7, 28 and 90 days, and 179, 200 and 262 for RC. Tables 4 and 5 show the results of the tests, in which the Spanish UNE [21–33] and ASTM standards were used. Each value in the table is the average of two tests for physical properties and an average of three for the mechanical tests (two for shrinkage and creep).

The sections below provide a summary of the behavior of the physical and mechanical properties.

2.4.1. Physical properties

The absorption of the RC increases proportionally with RCA content, while the density decreases slightly. Water porosity, like absorption, increases proportionally with RCA content. The above comments are presented in Table 4.

2.4.2. Mechanical properties

Simple compression decreases as the r factor increases for the studied ages: when $r \leq 0.30$, f'_c is appreciably the same as the reference concrete, and if the evolution of f'_c is compared with the age of the RC, it is seen that its behavior is the same as the reference concrete, although the stress levels are of course lower. Indirect stress shows a similar evolution with age as with ordinary concretes. However, samples with $r=0.60$ and $r=1.00$ show tensile strength values that are appreciably lower than the rest of the studied concretes for the age range under study. Finally, comparing results without reference to the age of the test, Young's modulus shows its minimum value for $r=0.60$, closely followed by the value for $r=1.00$. This property,

142
143
144
145
146
147
148
149
150
151
152
153
154
155
156
157
158
159
160
161
162
163
164
165
166
167
168
169
170
171
172
173
174
175
176
177
178
179
180
181
182

t5.1 Table 5
t5.2 Shrinkage and creep of RC

t5.3 Component properties	$r=1.00$	$r=0.60$	$r=0.30$	$r=0.15$	$r=0.00$	OC	
t5.4 f'_c (28 days) (MPa)	34.5	35.8	37.0	38.1	38.8	38.4 ^a	
t5.5 Stress level for creep (MPa) ^b	12.08	12.53	12.95	13.34	13.58	13.44	
t5.6 ϵ_{sh} basic (mm/m)	0.0138	0.0310	-0.0040	-0.0800	-0.0220	-0.0260 ^c	
t5.7 ϵ_{sh} drying (mm/m)	0.4029	0.4104	0.3524	0.3763	0.3740	0.1940 ^c	
t5.8 ϵ_c basic	Instantaneous (mm/m)	0.1370	0.1470	0.1645	0.1350	0.1430	0.1180 ^c
t5.9 φ (90 _{days} , t_0)	0.85	0.72	0.55	0.81	0.44	0.34 ^c	
t5.10 ϵ_c drying	Instantaneous (mm/m)	0.1580	0.1530	0.1380	0.1350	0.1600	0.1265 ^c
t5.11 φ (90 _{days} , t_0)	4.04	3.85	3.65	3.55	2.90	1.67 ^c	

t5.12 ^a The age of the test was 200 days.
t5.13 ^b $0.35f'_c$.
t5.14 ^c Shrinkage (262 and 172 days) and φ (262 and 172 days).

183 therefore, shows a similar behavior to ordinary concretes
184 (see Table 4).

185 For the shrinkage and creep tests, the samples, after
186 28 days in a curing chamber ($T=20\pm 2$ °C and RH=
187 $90\pm 5\%$), were submitted to a climatic chamber ($T=20$ °C
188 and RH=50%) for 90 days. The specimens used for basic
189 shrinkage and creep measurement were sealed with paraffin
190 (± 0.03 m thick) and wrapped in three layers of aluminum
191 foil. The details of these tests have been published by the
192 authors [17,18].

193 Table 5 presents the results of this experimental cam-
194 paign. This table shows the increase in the strain due to
195 shrinkage when the RCA increases its RC content. Simi-
196 larly, from these results, it is concluded that the creep
197 coefficients report a direct correlation with the increase of
198 the factor r (principally in shrinkage and creep for drying).

199
200 **2.5. Porosimetry by mercury intrusion**

201 Due to the broad pore size spectrum of the concretes
202 (1 nm–1 cm), it was decided to use the MIP technique,

203 which covers this spectrum to a great extent. It was applied
204 using the ASTM D 4404 standard [34] and the concepts
205 expressed below.

206
207 **2.5.1. Procedure**

208 The tests were carried out at 7, 28 (samples of concrete
209 submitted to curing chamber conditions to correlate them
210 with physical and mechanical properties of RCs) and 90 days
211 (samples of concrete submitted to climatic chamber condi-
212 tions to correlate them with shrinkage and creep). The
213 samples for the MIP tests were extracted from the center of
214 the samples (0.10 × 0.10 m) using a core catcher with a
215 diamond bit. The resulting cylinder ($\emptyset=0.02$ m × h=0.10 m)
216 was then cut with a fine saw to obtain two central cylinders
217 with dimensions of $\emptyset=0.02$ m × h=0.03 m.

218 The samples for tests at 7 and 28 days were dried by
219 stages: firstly, the samples were dehydrated by submerging
220 them in alcohol for 8 days. The alcohol was changed every
221 24 h. After this stage, the samples were dried by putting
222 them in an oven at $T=70$ °C for 24 h. Finally, the samples
223 were put into a drier until the tests.

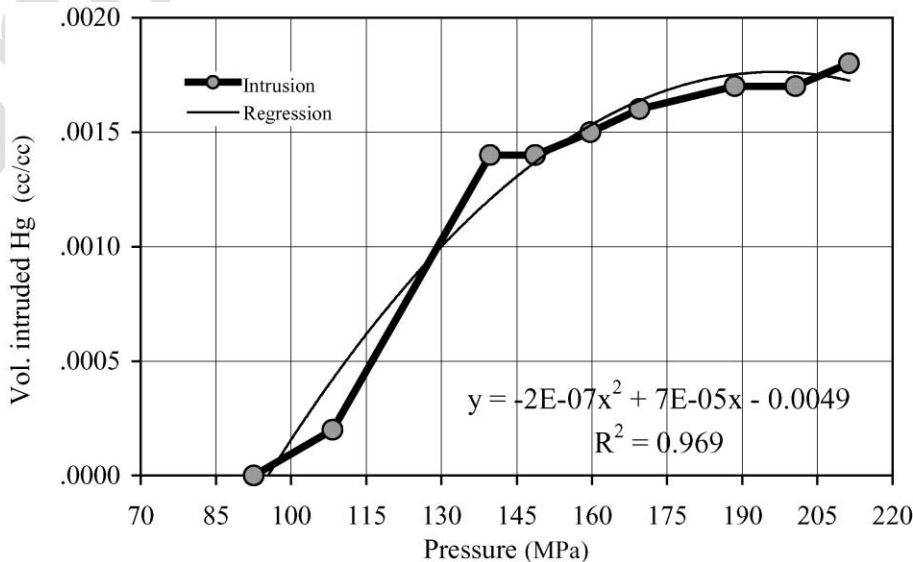


Fig. 1. Distribution in the black test.

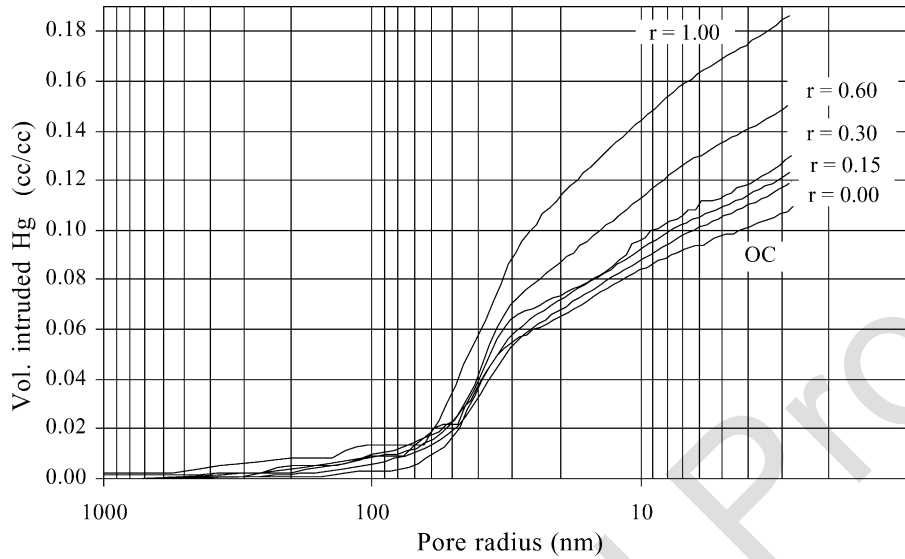


Fig. 2. General distribution (age 7 days).

224 The samples for the tests at 90 days, after 28 days in the
 225 curing chamber, were put in the climatic chamber until the
 226 age of 90 days. Upon arriving at this age, the samples were
 227 extracted and dried by putting them in an oven at $T = 120\text{ }^{\circ}\text{C}$
 228 for 24 h, and then in a drier.

229 The MIP tests were done on a Quantachrome Autoscan
 230 33 porosimeter, which subjected the samples to a maximum
 231 pressure of up to 226 MPa. The following parameter was
 232 measured: the theoretical pore radius (r_{pt}), within the range
 233 27–59,000 Å (the Washburn equation was used for the
 234 calculation). The process included the typical intrusion and
 235 extrusion cycles in this type of test. Finally, to improve the
 236 profile of the test curve, the sample results were filtered
 237 using a moving average with Base 9.

238 The following constants and hypotheses were applied
 239 in this study (for all the samples): mercury (Hg) contact
 240 angle with the concrete $\theta = 130^{\circ}$, Hg surface tension
 241 $\sigma = 0.480\text{ N/m}^2$, pore shape factor $\varphi = 4.00$, together
 242 with the typical hypotheses of the methodology of this
 243 test [35,36].
 244

245 2.5.2. Corrections applied to the test values [37]

246 The test values obtained based above were submitted to
 247 three corrections to improve their accuracy.
 248

249 2.5.2.1. *Blank test.* A test with the dilatometer without a
 250 sample was carried out to obtain the volume of Hg that
 251 causes the dilatometer to expand, and the compression that

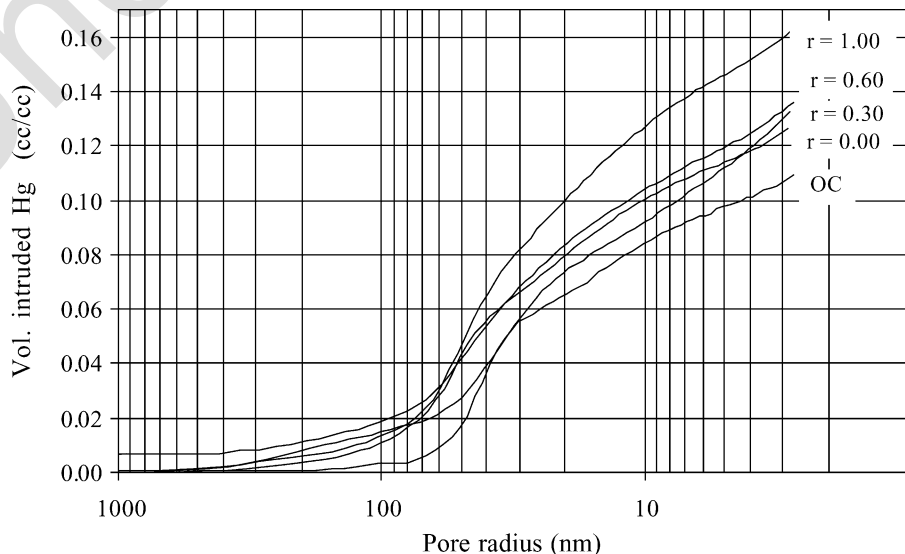


Fig. 3. General distribution (age 28 days).

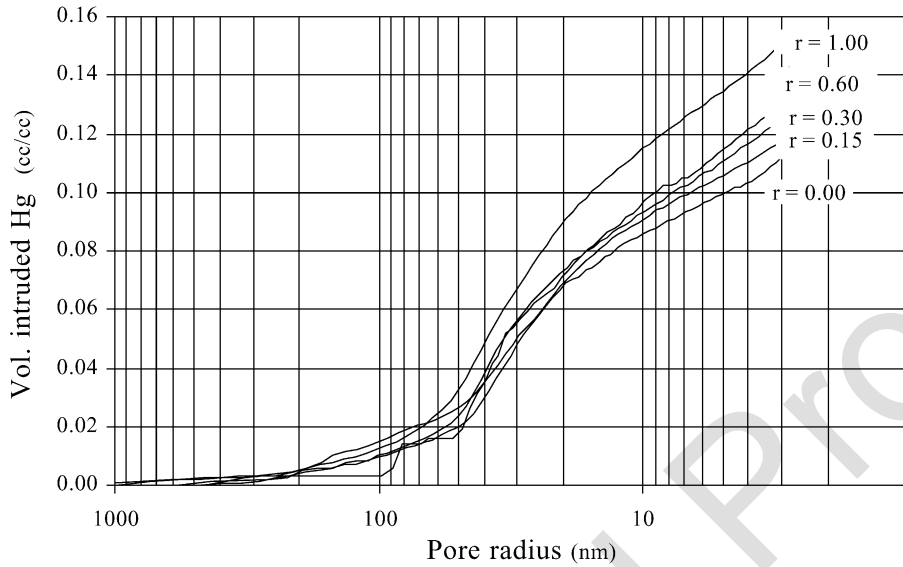


Fig. 4. General distribution (age 90 days).

252 the Hg undergoes to fill the dilatometer. The following
 253 correlation was obtained from this test (see Eq. (1)):

$$V_{\text{blank}} = -2E^{-07}x^2 + 7E^{-05}x - 0.0049. \quad (1)$$

254 The result of the above correlation (V_{blank}) was subtracted
 256 from the uncorrected Hg volume of the tests (V_o) when the
 257 test pressure (x) was greater than or equal to 92.56 MPa. The
 258 blank test and the proposed correlation are shown in Fig. 1.
 259

260 **2.5.2.2. Differential compression of Hg.** The sample dis-
 261 places a volume of Hg equal to the mass of the sample
 262 (BV_{sample}). The blank test, therefore, includes the compres-
 263 sion of a volume of mercury (equal to BV_{sample}) that is not
 264 seen in the volume of the experimental test (V''_{cHg}). If the

above variables are taken into account, it is possible to
 265 determine V''_{cHg} using the following equation (Eq. (2)):
 266

$$V''_{\text{cHg}} = 0.175BV_{\text{sample}}\log_{10}(1 + (x/1820 \text{ MPa})). \quad (2)$$

267
 268
 269
2.5.2.3. Compression of the sample. This estimates the
 270 compressibility factor of a volume of the sample that was
 271 not intruded (V_{cs}). Given the compressibility coefficient of
 272 the material (ψ_{sample} , proposed = $5.0 \text{ E}^{-10} \text{ m}^2/\text{N}$) and the
 273 volume of the sample without intruded Hg (UV_{sample}), it is
 274 feasible to calculate the compression of the sample using the
 275 following equation (Eq. (3)):
 276

$$V_{\text{cs}} = x\psi_{\text{sample}}UV_{\text{sample}}. \quad (3)$$

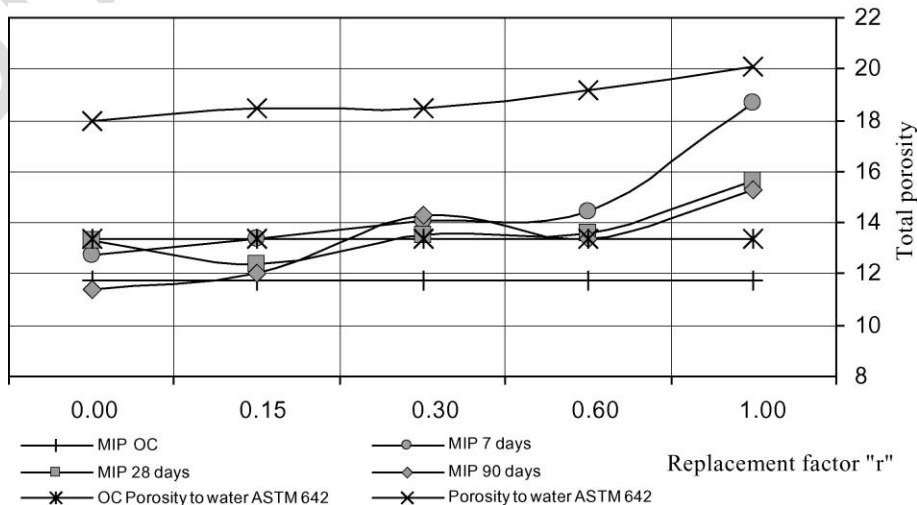


Fig. 5. Total porosity.

t6.1 Table 6
t6.2 Critical radius for the different RCs

t6.3 r_{critical} (nm)	t6.4 dv/dp VS pore radius			t6.5 $\alpha^a > 1'$			t6.5 $1' < \alpha^a < 5'$		
t6.5 Method factor	7 days	28 days	90 days	7 days	28 days	90 days	7 days	28 days	90 days
t6.6 OC	44.70	–	–	63.64 ^b	–	–	57.34 ^b	–	–
t6.7 $r=0.00$	40.31	51.61	38.53	70.39	83.93	62.67	59.76	68.75	51.94
t6.8 $r=0.15$	36.50	73.63	40.60	65.17	68.68	57.26	56.21	47.63	46.46
t6.9 $r=0.30$	53.88	91.62	40.96	65.50	69.50	67.04	60.15	60.98	56.95
t6.10 $r=0.60$	44.45	51.00	48.75	70.01	79.48	97.39	60.24	55.78	93.36
t6.11 $r=1.00$	45.87	49.63	43.68	68.78	74.29	78.78	58.40	65.66	64.48
t6.12 Maximum	53.88	91.62	48.75	70.39	83.93	97.39	60.24	68.75	93.36
t6.13 Minimum	36.50	49.63	38.53	63.64	68.68	57.26	56.21	47.63	46.46
t6.14 Average	44.28	63.50	42.50	67.25	75.71	72.63	58.68	59.76	62.64

t6.15 ^a Angle between two consecutive points (pore radius – volume intruded Hg).

t6.16 ^b At 262 days of age.

278 The final equation that was used to calculate the porosity at
279 each point of the tests according to the above corrections
280 was the following (see Eq. (4)):

$$281 \quad V_{\text{intrusion}} = V_o - V_{\text{blank}} + V''_{\text{cHg}} - V_{\text{cs}} \quad (4)$$

282

283

284 2.5.3. Results

285 The following sections present the results and analyses
286 derived from the MIP tests performed on the various
287 concretes in the study.

288

289 2.5.3.1. *Distribution of the pore radius.* Figs. 2–4 show
290 the graphs for the tests carried out at 7, 28 and 90 days for
291 the various concrete samples. To avoid confusion when
292 interpreting the graphs, only the curves of the Hg intrusion
293 stages are presented.

294 It may be seen from the three graphs that the increase in
295 the r factor of the RCs shows a correlation with total
296 porosity, as the latter increases by 5.9% when r goes from
297 $r=0.00$ to $r=1.00$ at 7 days, 2.3% for 28 days and 3.8% for
298 90 days (taken from the three graphs as average values of
299 two tests for each variable).

300 It is also seen in Fig. 5 that the total porosity
301 decreases appreciably for all the concretes as a function
302 of age. The evolution of total porosity of these concretes
303 amounts to a decrease of 0.5% from 7 to 28 days with
304 the exception of $r=1.00$, which shows a greater reduction
305 (3.0%). Total porosity drops by 0.42% on average upon
306 going from 28 to 90 days, the maximum standing at
307 $r=1.00$ (1.9%).

308 It should be pointed out that the main difference in the
309 total porosity between the different RCs ($r=1.00$ and the
310 rest of the concretes) is seen in the area with pore radius less
311 than 30 nm (the zone of maximum percentage of pore
312 volume in the concretes and originating in the cement
313 mortar). It is also in this zone that the decrease in porosity
314 with age is seen. The above pore range is commonly
315 associated with the power to damage the dimensional

stability and influence the mechanical properties of the
concretes [38].

2.5.3.2. *Critical pore radius.* Characteristic radius or crit-
ical pore (r_{critical}) is the term given to the corresponding
radius that causes the beginning of the maximum slope in
the curve of the radius versus volume of the intruded Hg
graph. This pore radius is usually an indicator of the
microstructure of the material and it is used to detect a
variety of materials. For the determination of this parameter,
two different methods were used as follows:

(i) Calculate the angle between two consecutive points
(α) of all the values that take in all of the curves in the study.
The criteria for establish distinction were the following: (a)
pore radius that causes the first angle that is greater than 1°
of elevation in the slope of the curve under study; and (b)
the average pore radius range that generates an angle of
elevation between 1° and 5° of the beginning of elevation of
the curve under study.

(ii) Point maximum peak of the named curve of frequen-
cies density dv/dp ($\text{cm}^3/\text{MPa cm}^3$) VS pore radio (nm).

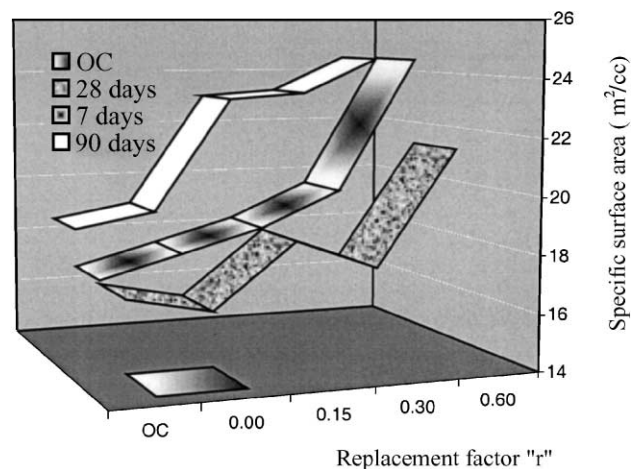


Fig. 6. Specific surface area for RC.

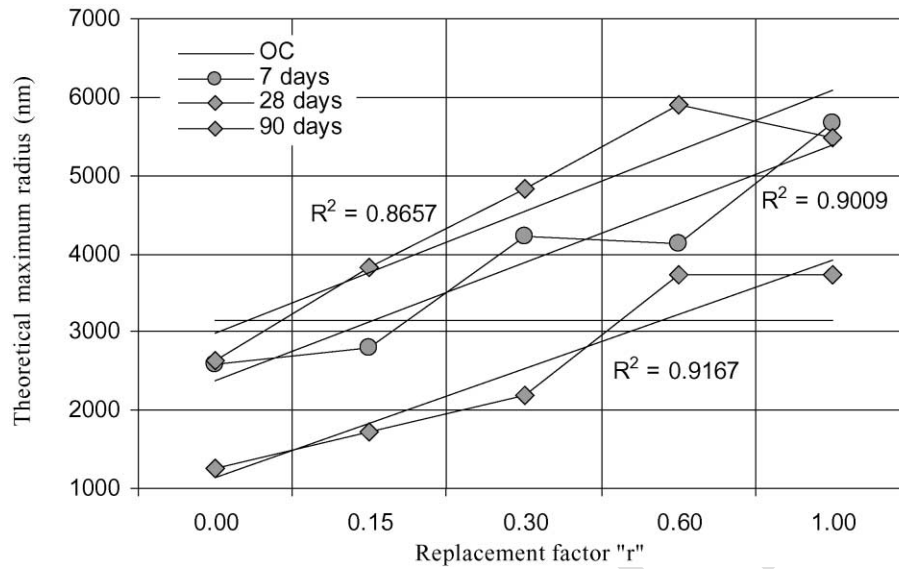


Fig. 7. Maximum pore radius.

337 Table 6 shows the critical pore radius calculated as
 338 explained above. As is seen, the values in the tests are
 339 approximately 36–97 nm (with a population average of
 340 60.46 nm), which locates these pores in the range of large
 341 capillary or macropores (50–10,000 nm); at this capillary
 342 range, negative effects that can affect the strength and the
 343 impermeability of a concrete can be attributed to the pore
 344 size. However, the difference between the different $r_{critical}$ of
 345 the concretes studied is negligible as the variation between
 346 them is small. With respect to the two methods for its
 347 determination, the most exact is critical pore radius; how-
 348 ever, Case (i,b) is of greater importance due to the ease with
 349 which it determines $r_{critical}$ and the fact that it presents a mean
 350 variation with respect to critical pore radius of only 15%.

2.5.3.3. *Specific surface area.* The MIP technique ena-
 351 bles the determination of the surface area of the material
 352 from direct sampling of the pressure versus volume of
 353 intruded Hg (Fig. 6). The method does not require pre-
 354 vious knowledge of the geometry of the pore, which
 355 means that its results are reliable. However, the maximum
 356 level of available pressure of the porosimeter used cannot
 357 guarantee intrusion of all the pore sizes that cover the
 358 specific surface of the samples and it is not possible to
 359 evaluate whether high levels of pressure cause crushing of
 360 sealed pores.
 361

The observed general behavior is an increase (import-
 362 ant for the case of $r=1.00$) in agreement with the
 363 increase of the r factor. For this property, the results do
 364
 365

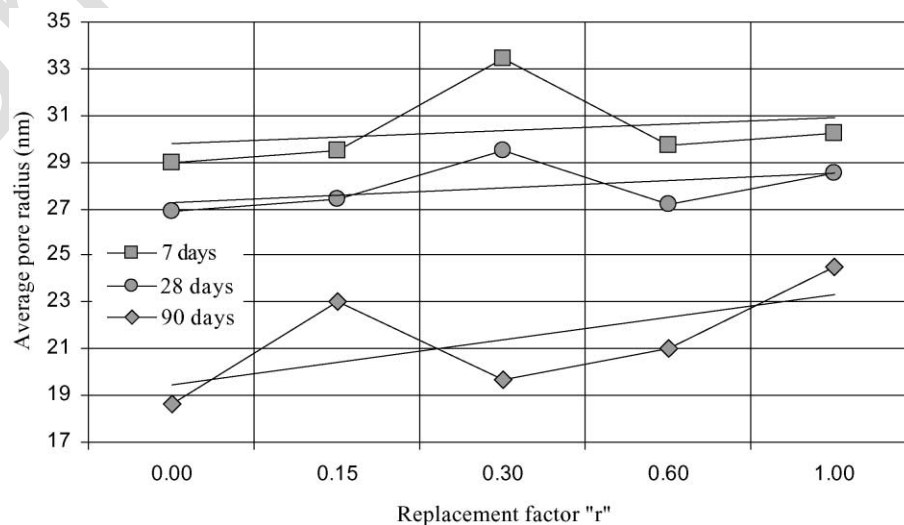


Fig. 8. Average pore radius.

t7.1 Table 7

t7.2 Correlation between total porosity and other properties of the RCs

t7.3 Property	Equation ^a	R ²
t7.4 Absorption (%)	$y = 0.3501x + 4.0460$.7641
t7.5 Porosity to water (%)	$y = 0.5714x + 11.036$.7000
t7.6 D_s (t/m ³)	$y = -0.0165x + 2.3514$.7267
t7.7 D_{sss} (t/m ³)	$y = -0.0191x + 2.5836$.7745
t7.8 Permeability (cm)		
t7.9 Average	$y = 0.1564x - 1.3955$.7652
t7.10 Maximum	$y = 1.0006x - 1.3819$.6076
t7.11 f_t (MPa)	$y = 0.0185x^2 - 0.6527x + 8.9077$.5727
t7.12 f_c' (MPa)	$y = 0.3744x^2 - 12.906x + 141.05$.7350
t7.13 E (GPa)	$y = 0.1984x^2 - 6.395x + 77.316$.6510
t7.14 ϵ_{sh} drying (mm/m)	$y = 2E - 08z^2 - 9E - 05z + 0.4607$.8367
t7.15 φ (90 days, t_0)	$y = -3E - 07z^2 + 0.0019z + 1.0833$.9347

t7.16 ^a x = total porosity in (%) MIP; z = pore threshold (nm).

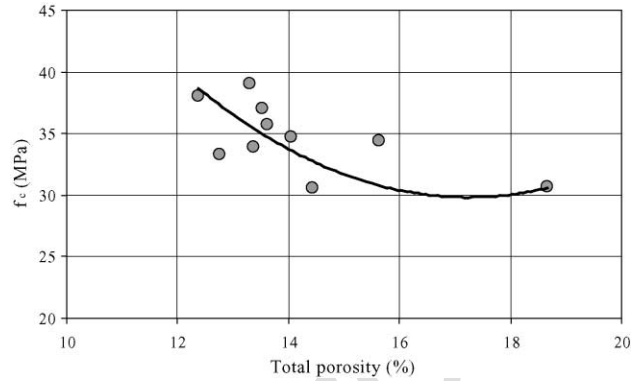


Fig. 10. Total porosity versus compressive strength.

366 not present a logical correlation with the age of the speci-
 367 mens, which maybe related to the fact that the samples were
 368 submitted to two types of environmental conditions and two
 369 drying processes.

370
 371 **2.5.3.4. Pore threshold.** This name is given to the
 372 maximum pore radius found (either in the intrusion or
 373 extrusion stage) in the MIP test [39]. Fig. 7 shows the
 374 maximum radius for the concretes studied.

375 Correlations for the three curves are fairly high. How-
 376 ever, the interpretation and usefulness of this parameter can
 377 only serve as a guideline, as its determination involves a
 378 high degree of uncertainty.

379
 380 **2.5.3.5. Average pore radius.** Pore radius ($r_{average}$) is the
 381 name given to the radius that corresponds to 50% of the
 382 total volume of Hg intruded in the test. In Fig. 8, the $r_{average}$
 383 calculated through the Lagrange interpolation of the two
 384 nearest points to 50% of the total volume for each sample
 385 is presented.

386 The presented behavior of $r_{average}$ is correlative with the
 387 age of the samples, as well as with the r factor (in this last
 388 case in smaller proportion).

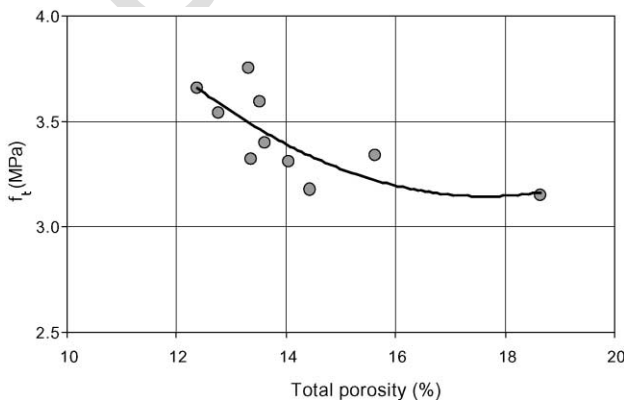


Fig. 9. Total porosity versus tensile strength.

389
 390 **2.5.4. Correlation between porosity and properties of the**
 391 **concretes**

392 The correlation process was carried out on the properties
 393 obtained from the MIP tests, the physical and mechanical
 394 properties of the RCs (7 and 28 days), and shrinkage and
 395 creep (90 days). The processed data were examined with
 396 different lines of tendency, in which different correlation
 397 coefficients (R^2) were used as indicators of greater recip-
 398 rocity between the variables.

399 Table 7 shows the correlation equations for the total
 400 porosity data and the physical properties of the RCs. The
 401 correlations only include MIP tests for 28 days, as the
 402 physical tests were done at this time. The table also shows
 403 the correlation for total porosity and mechanical prop-
 404 erties of the RCs (the correlations are an average of tests at 7
 405 and 28 days). Finally, the correlation equations between shrink-
 406 age and the creep coefficient with the MIP tests for 90 days
 407 are also presented.

408 Figs. 9–11 show the graphs that gave rise to the
 409 correlations of the mechanical properties and the total
 410 porosity obtained in the MIP tests.

411 Total porosity, obtained from the MIP tests, is the
 412 property that showed the best correlation for the behavior

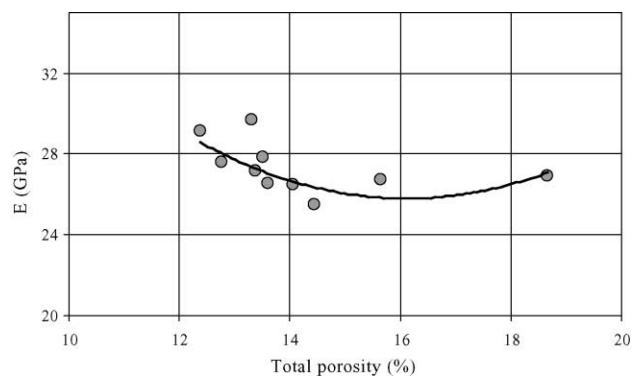


Fig. 11. Total porosity versus Young's modulus.

413 of the studied concretes, followed by the specific surface
414 area, r_{critical} , the pore threshold radius and, lastly, r_{average} .

415 As regards the types of lines of tendency used, the
416 physical properties follow the pattern of linear correlation
417 better than the mechanical properties, while the mechanical
418 properties fit quadratic-type equations better. This latter fact
419 may indicate that these equations could be improved if other
420 factors (in addition to total porosity) of similar importance
421 are taken into account, such as the increase in the interface
422 zones (which favors the formation and propagation of micro-
423 cracks) and a major variation in the distribution of the pore
424 radius (especially in the zone of pore radius <30 nm). In
425 both cases, the cause of these new factors to be considered in
426 RCs is the old mortar that adheres to the NA of which the
427 RCA is composed.

428 3. Conclusions

429 Based on the research and results presented in this paper,
430 the following conclusions are reached.

431 • The replacement factor r of the RCs shows a correla-
432 tion with total volume and pore size, its influence being
433 more important at lower ages and diminishing as the
434 concrete ages. This influence is attributed to the crystalliza-
435 tion of new products that reduce both the number and size
436 of the pores.

437 • The most significant differences of the studied samples
438 are seen in two parameters: (1) the greater pore radius
439 threshold as the replacement of NA by RCA is increased;
440 and (2) the detection of zones of major quantitative changes
441 seen in the increase of the pore volume from pores with
442 radius <30 nm.

443 • The effect of the r factor does not seem to influence the
444 r_{critical} values, and therefore, this parameter may be used
445 only in cases in which determination of the variation of
446 structural components of the concrete that was used for the
447 RCA is desired, and whose probable cause of variation
448 would be the modification of the physical constants of the
449 concretes (W/C, type of cement, etc.).

450 • The results for specific surface area, together with total
451 porosity, are those which better describe and correlate the
452 results of the properties of the studied concrete. However, it
453 will be necessary to supplement this information with tests
454 of gas absorption, which would enable quantification of the
455 surface area in the micropore zone and thus be able to
456 better correlate these tests with other properties such as
457 shrinkage and creep; both are linked to the distribution and
458 quantity of micropores.

459 • Finally, correlation between the properties of the RC
460 and total porosity is difficult to determine. However, it
461 would be feasible to improve it if the distribution of the
462 pore radius was included. This distribution could be ascer-
463 tained by classifying boundaries between different ranges of
464 pore size, taking as a classification criterion the effect of
465 size on the behavior of the property of the RC under study.

It would also be advisable to include parameters that 466
evaluate the formation and propagation of microcracks in 467
the interface zones, as these zones (mechanically weaker 468
than the mortar) increase in the RCs due to the replacement 469
of NA by RCA. 470

Acknowledgments 471

The author would like to express their gratitude to the 472
company Cervezas Finas de Cd. Serdán, Puebla, Mexico, 473
for the partial financing of this research; to the Technical 474
University of Catalonia, Barcelona, Spain, for the use of 475
their facilities; and to Drs. L. Agulló and E. Vázquez. 476

References 477

- [1] J. Björn-Jakobse, M. Elle, E.K. Lauritzen, On-site use of regenerated 478
demolition debris, in: Y. Kasai (Ed.), *Demolition and Reuse of Concrete* 479
and Masonry, Reuse of Demolition Waste, vol. 2, 1988, pp. 537–546. 480
- [2] W. Grübl, *Environmentally Friendly Construction Technology—Inter-* 481
action Between Construction and Environment (1999) ([http://www.b-i-](http://www.b-i-m-de/public/Tudmassiv/dacon98gruebl.htm) 482
[m-de/public/Tudmassiv/dacon98gruebl.htm](http://www.b-i-m-de/public/Tudmassiv/dacon98gruebl.htm)). 483
- [3] T.C. Hansen, *Recycled of demolished concrete and masonry*, Report 484
of Technical Committee 37-DRC *Demolition and Reuse of Concrete*, 485
Part 1 (1992) 1–160. 486
- [4] T.C. Hansen, E. Bøgh, *Elasticity and drying shrinkage of recycle-* 487
aggregate, *ACI J.* (5) (1995) 648–652. 488
- [5] T.C. Hansen, M. Marga, *Strength of recycle made from coarse and* 489
fine recycled concrete aggregates, in: Y. Kasai (Ed.), *Demolition and* 490
Reuse of Concrete and Masonry, Reuse of Demolition Waste, vol. 2, 491
1988, pp. 605–612. 492
- [6] M. Kakizaki, M. Harada, T. Soshiroda, S. Kubota, T. Ikeda, Y. Kasai, 493
Strength and elastic modulus of recycled aggregate concrete, in: Y. 494
Kasai (Ed.), *Demolition and Reuse of Concrete and Masonry, Reuse* 495
of Demolition Waste, vol. 2, 1988, pp. 565–574. 496
- [7] E.K. Lauritzen, M. Jannerup, *Guidelines and experience from the* 497
demolition of houses in connection with the resound Link between 498
Denmark and Sweden, Demolition and Reuse of Concrete and 499
Masonry, in: E.K. Lauritzen (Ed.), *Guidelines for Demolition and Reuse* 500
of Concrete and Masonry, pp. 35–46. 501
- [8] P.J. Wainwright, A. Trevorrow, Y. Yu, Y. Wang, *Modifying the per-* 502
formance of concrete made with coarse and fine recycled concrete 503
aggregates, in: E.K. Lauritzen (Ed.), *Demolition and Reuse of Con-* 504
crete and Masonry, Guidelines for Demolition and Reuse of Concrete 505
and Masonry, 1993, pp. 319–330. 506
- [9] A. Müller, A. Winkler, *Characteristics of processed concrete rubble*, 507
in: K.R. Dhir, N.A. Henderson, M.C. Limbachiya (Eds.), *Uses of* 508
Recycled Concrete Aggregate. Sustainable Construction, 1998, pp. 509
1109–1119. 510
- [10] P.J. Wainwright, J.G. Cabrera, *Use of demolition concrete to produce* 511
durable structural concrete, in: J.J.J.M. Goumans, H.A. Van Der Sloot, 512
T.G. Aalbers (Eds.), *Environmental Aspects of Construction with* 513
Waste Materials, 1994, pp. 553–562. 514
- [11] B. Zhang, *Relationship between pore structure and mechanical proper-* 515
ties of ordinary concrete under bending fatigue, *Cem. Concr. Res.* 28 516
(5) (1998) 699–711. 517
- [12] H. Uchikawa, S. Hanehara, *Recycling of concrete waste*, in: R.K. 518
Dhir, T.D. Dyer (Eds.), *Concrete for Environment Enhancement and* 519
Protection, 1996, pp. 163–172. 520
- [13] C.F. Hendriks, *Certification system for aggregates produced from* 521

- 522 building waste and demolished buildings, in: J.J.J.M. Goumans, H.A.
 523 Van Der Sloot, T.G. Aalbers (Eds.), *Environmental Aspects of Con-*
 524 *struction with Waste Materials*, Elsevier, Amsterdam, The Nether-
 525 lands, 1994, pp. 821–843.
- 526 [14] J. Kasai, Y., Guidelines and the present state of the reuse of demol-
 527 ished concrete in Japan, in: E.K. Lauritzen (Ed.), *Demolition and*
 528 *Reuse of Concrete and Masonry, Guidelines for Demolition and Reuse*
 529 *of Concrete and Masonry*, 1993, pp. 93–104 (Odense, Denmark).
- 530 [15] RILEM Recommendation, 121-DRG Guidance for demolition and
 531 reuse of concrete and masonry. Specifications for concrete with re-
 532 cycle aggregates, *J. Mater. Struct.* 27 (1994) 557–59.
- 533 [16] J. Vyncke, E. Rousseau, Recycling of construction and waste in Bel-
 534 gium: actual situation and future evolution, in: E.K. Lauritzen (Ed.),
 535 *Demolition and reuse of concrete and masonry, Guidelines for Dem-*
 536 *olition and Reuse of Concrete and Masonry*, 1993, pp. 57–69
 537 (Odense, Denmark).
- 538 [17] J.M. Gómez, E. Vázquez, L. Agulló, Strength and deformation proper-
 539 ties of recycled aggregate concrete, Fifth CANMET/ACI International
 540 Conference on Recent Advances in Concrete Technology, Singapore,
 541 2001, pp. 103–120 (Supplementary papers; M. Venturino (Compiler)).
- 542 [18] J.M. Gómez, L. Agulló, E. Vázquez, Cualidades físicas y mecánicas
 543 de los agregados reciclados de concreto. *Construcción y Tecnología.*
 544 *Magazine of the Mexican Institute of the Cement and the Concrete,*
 545 *AC (IMCYC), Mexico, DF, Mexico, Vol. XIII (157) (2001) pp. 10–*
 546 *22 (ISSN 0187-7895) (In Spanish) [http://www.imcyc.com/cyt/junio/](http://www.imcyc.com/cyt/junio/cualidades.htm)*
 547 *cualidades.htm.*
- 548 [19] J.M. Gómez, E. Vázquez, L. Agulló, Hormigón con áridos reciclados.
 549 Una guía de diseño para el material. International Center of Numerical
 550 Methods in Engineering (CIMNE). Monograph M60 (2001) 1–137
 551 (ISBN 84-89925-80-1), Barcelona, Spain (in Spanish).
- 552 [20] J.M. Gómez, L. Aguyó, E. Vázquez, Repercussions on concrete per-
 553 meability due to recycled concrete aggregate, in: V.M. Malhotra (Ed.),
 554 *Third CANMET/ACI International Symposium on Sustainable Develop-*
 555 *ment of Cement and Concrete*, San Francisco, USA, 2001, pp.
 556 181–195 (ISBN 0-87031-041-0; SP 202–13).
- 557 [21] UNE 7083, Determinación del peso específico y de la absorción en
 558 gravas y arenas, AENOR (Asociación Española de Normalización y
 559 Certificación), 1954 (in Spanish).
- 560 [22] UNE 7140, Determinación de los pesos específicos y absorción de
 561 agua en áridos finos, AENOR (Asociación Española de Normaliza-
 562 ción y Certificación), 1958 (in Spanish).
- 563 [23] UNE 7238, Determinación de coeficiente de forma del árido grueso
 564 empleado en la fabricación de hormigones, AENOR (Asociación Es-
 565 pañola de Normalización y Certificación) (in Spanish).
- 566 [24] UNE 83.116, Áridos para hormigón, Determinación del coeficiente
 567 Los Ángeles, AENOR (Asociación Española de Normalización y Cer-
 568 tificación), 1990 (in Spanish).
- 569 [25] UNE 83.131, Áridos para hormigones, Determinación del equivalente
 de arena, AENOR (Asociación Española de Normalización y Certif-
 icación), 1990 (in Spanish).
- [26] UNE 83.133, Áridos para hormigones, Determinación de las densi-
 dades, coeficientes de absorción y contenido de agua en el árido fino,
 AENOR (Asociación Española de Normalización y Certificación),
 1990 (in Spanish).
- [27] UNE 83.134, Áridos para hormigones, Determinación de la densidad,
 porosidad, coeficiente de absorción y contenido en agua del árido
 grueso, AENOR (Asociación Española de Normalización y Certifica-
 ción), 1990 (in Spanish).
- [28] UNE 83.304, Ensayos de hormigón, Rotura por compresión, AENOR
 (Asociación Española de Normalización y Certificación), 1984 (in
 Spanish).
- [29] UNE 83.306, Ensayos de hormigón, Rotura por tracción indirecta
 (Ensayo Brasileño), AENOR (Asociación Española de Normalización
 y Certificación), 1985 (in Spanish).
- [30] UNE 83.310, Ensayos de hormigón, Determinación de la permeabili-
 dad, AENOR (Asociación Española de Normalización y Certifica-
 ción), 1990 (in Spanish).
- [31] UNE 83.312, Ensayos de hormigón. Hormigón endurecido, Determi-
 nación de la densidad, AENOR (Asociación Española de Normaliza-
 ción y Certificación) 1990 (in Spanish).
- [32] UNE 83.316, Ensayos de hormigón, Determinación del módulo de
 elasticidad en compresión, AENOR (Asociación Española de Normal-
 ización y Certificación), 1996 (in Spanish).
- [33] UNE-EN 933:3, Ensayos para determinar las propiedades mecánicas y
 físicas de los áridos: Parte 3. Determinación de la forma de las particu-
 las. Índice de lajas, AENOR (Asociación Española de Normalización
 y Certificación), 1997 (in Spanish).
- [34] ASTM D 4404, Determination of pore volume and pore volume dis-
 tribution of soil and rock by mercury intrusion porosimetry.
- [35] F.G. Rodríguez, Porosimetría por intrusión de mercurio: Fundamentos
 de la técnica y aplicación a la caracterización microestructural de
 hormigones, *Ing. Civ.* (1997) 21–37 (in Spanish).
- [36] S. Diamond, Methodologies of PSD measurements in HCP: Postu-
 lates, peculiarities, and problems, in: L.R. Roberts, J.P. Skalny
 (Eds.), *Pore Structure and Permeability of Cementitious Materials,*
Symposium Proceedings, vol. 137, Materials Research Society,
 1989, pp. 83–89.
- [37] A. Raymond, A. Cook, K.C. Hover, Mercury porosimetry of cement-
 based materials and associated correction factors, *ACI Mat. J.* (1993)
 152–161.
- [38] D.A. St. John, A.W. Poole, I. Sims, *Concrete petrography, A Hand-*
book of Investigative Techniques, Arnold, 1998, pp. 1–474.
- [39] R.F. Feldman, The porosity and pore structure of hydrated Portland
 cement paste, in: L.R. Roberts, J.P. Skalny (Eds.), *Pore Structure and*
Permeability of Cementitious Materials, Symposium Proceedings, vol.
 137, Materials Research Society, 1989, pp. 59–73.